Continuous Behavioral State Modeling via HMM for Adherence Recognition in Psychoeducational Intervention Processes

Jiayang Li
School of Nursing, Hebi Polytechnic, Hebi 458030, Henan, China
Corresponding author: Jiayang Li (e-mail: ljy1234567892025@126.com)

ABSTRACT Current compliance identification methods in psychoeducational interventions often rely on discrete retrospective assessment and cannot dynamically capture continuous state evolution. To address this limitation, this paper proposes a continuous behavioral state modeling method based on the Hidden Markov Model. Real-time user interaction behavior sequences are collected through a digital intervention platform and used as observation data. Potential internal compliance states are defined according to psychoeducational theory, and the probabilistic relationship between observed sequences and latent states is modeled using HMM. Through parameter learning of state transition and observation probabilities and decoding algorithms, the user's real-time compliance state sequence is dynamically inferred, enabling continuous and automated tracking of compliance levels. Experimental results show that the proposed method is highly consistent with expert annotations in identifying turning points, achieving a state sequence alignment accuracy of 0.833, outperforming random forest and rule-based methods. For early warning, the model detects "significantly decreased compliance" and "intervention dropout" events 12.5 and 18.2 days earlier on average, with recall of 0.900 and AUC of 0.892.

INDEX TERMS hidden markov model, psychoeducational intervention, compliance recognition, continuous behavior modeling, early warning

I. INTRODUCTION

AS a prominent preventive and promotional tool, psychoeducational intervention focuses on providing systematic training in psychological adjustment via knowledge transfer, skill development (training), and cognitive restructuring. The advanced integration of digital technology has resulted in the gradual evolution of psychoeducational intervention from a one-time, static offline model to an ongoing, dynamic, and interactive online activity. The level of ongoing participation and engagement on the part of the user—i.e., "intervention compliance"—is now recognized as a crucial process contributing to overall effectiveness of the intervention itself.

At present, the primary means of identifying compliance during a psychoeducational intervention uses retrospective evaluations through phase-sensitive self-report measures or interviews. The retrospective design of these methods restricts their ability to determine the length of time to conduct the evaluation, produces a significant level of subjectivity, and does not permit capturing the fluctuation in compliance that occurs throughout the intervention process [1,2]. There have also been several studies that utilized digital methods to collect behavioral data to enhance the objectivity and timeliness of compliance's evaluation. Still, nearly all digital methodologies utilize static feature identification or time-point hydraulic classification for their analyses [3,4]. However, very few methods have developed a valid modeling method for the continuous nature of behavioral evolution [5,6]. Also, although traditional measures may yield some degree of validity in selected situations, their retrospective nature makes them ineffective for providing timely projections and coordinating intervention modifications in an immediate manner [7,8]. Moreover, achieving continuous, dynamic, and interpretable automated identification of compliance status remains a key challenge for current research. For continuous modeling of behavioral states, time-series probabilistic models have shown unique value. Hidden Markov Models (HMMs) are powerful in behavioral analysis, health monitoring and other fields because they can describe the probability transition of hidden states over time [9,10]. At the methodological level, multilevel HMMs [11] and Bayesian multilevel HMMs [12] provide a more flexible modeling framework for processing complex behavioral data, while reasoning optimization based on expert knowledge [13] also enhances the interpretability and adaptability of the model. At the application level, some studies have shown that HMMs have been widely used in learning engagement modeling [14], daily activity identification [15], user participation dynamic analysis [16], internal threat detection [17], mental health status prediction [18,19], and dependency evolution early warning [20]. In addition, related time-series models such as Markovmodulated Hawkes processes have also shown potential in modeling sudden behavioral events [21]. However, in the field of psychological intervention, although some studies have attempted to analyze behavioral patterns using hybrid Markov models or model human-computer collaboration dynamics using HMMs, no systematic work has yet applied HMMs to the continuous compliance state modeling and real-time identification in the psychological education intervention process [22,23]. Existing methods generally lack the ability to explicitly model the continuous evolution of behavioral states, which is the core of achieving dynamic and refined compliance assessment.

Therefore, this paper aims to address the key problem of the difficulty in dynamically and continuously identifying compliance in the psychological education intervention process, focusing on achieving continuous behavioral state modeling through HMMs. The study adopts an HMM-based modeling framework, defining three potential compliance states—"high," "medium," and "low"—based on psychological education theory. User behavior sequences collected from a digital platform are used as observations. The Baum-Welch algorithm estimates state transition and observation probabilities. The Viterbi algorithm then decodes the most probable sequence of hidden states from the observed behavior stream, producing a real-time, time-stamped trajectory of the user's compliance level throughout the intervention. This paper's major contribution is the definition of a number of potential states with distinct psychological significance while providing the ability to carry out probabilistic modeling and decoding continuously using HMM. This will allow real-time, dynamic, and automatic tracking of an individual's compliance to an intervention during a psychoeducation intervention process, and additionally allow a new way to assess and adjust digital interventions.

II. COMPLIANCE STATE MODELING AND RECOGNITION METHOD BASED ON HIDDEN MARKOV MODELS

A. DIGITAL PLATFORM BEHAVIORAL DATA COLLECTION AND OBSERVATION SEQUENCE CONSTRUCTION

The information contained within this document originates from a standardized digital intervention platform for mental health that delivers psychologic educational content through a digital platform (e-learning platform). This is accomplished through the backend/staging system for logging all interactions that using the e-learning system, providing the user with access therapeutic content, representing the user's learning progress as they work through each class/module, details of assigned practice tasks that were completed, as well as the frequency of returning to previously completed modules. User data is captured session by session in order to capture the continuing evolution of the user experience, maintained as long as they remain engaged with the platform.

The behavioral data generated by a single user during a complete intervention session are organized temporally to construct the observation sequence required for the Hidden Markov Model (HMM) [24,25], as shown in Figure 1.

In Figure 1, it can be seen that the cleaning and preprocessing of raw log data to eliminate noise records that result from network latency/mis-operation/system failure. Based on cleaned log data, a multidimensional behavioral feature set was extracted according to the framework for analyzing the psychoeducational intervention process. The extracted features allow this paper to quantitatively measure the quality and nature of how a user participates within program. Some important dimensions of user behaviour are: click frequency (the number of interactions which occur on average per time unit); dwell time (the time spent actively engaging with specific content within our intervention); task completion rate (the percentage of assigned exercises/tasks completed by a user; and interaction depth (the amount of content accessed). Each feature is normalized and discretized to adapt to subsequent model input requirements.

Specifically, user behavior is sliced using fixed time windows or key intervention event nodes. To accommodate variability in user interaction frequency, empty time windows resulting from periods of inactivity are assigned a designated observation symbol representing absence of engagement, ensuring that the observation sequence maintains a consistent temporal resolution without introducing bias into state transition estimation. This process employs a sliding time window approach, as depicted in Figure 1. The multidimensional behavioral feature values within each time slice are vectorized, and the vector is transformed into a discrete observation symbol using predefined symbol mapping rules. Finally, these observation symbols are arranged chronologically to form an observation sequence representing the user's behavioral pattern. This sequence serves as input to the HMM to characterize the user's explicit interactive behavior evolving over time.

B. THEORETICAL DEFINITION OF LATENT COMPLIANCE STATES AND INITIALIZATION OF LATENT STATE SPACE

In the Hidden Model (HMM) framework, latent states represent the user's inherent psychological attributes that cannot be directly observed [26,27]. This paper operationalizes "intervention compliance" as the psychological and behavioral tendency of users to consistently, proactively, and with high quality follow a pre-set intervention plan. To model this, based on mature theories of behavioral change stages and engagement in the field of psychoeducation, this continuous internal construct is discretized into a finite

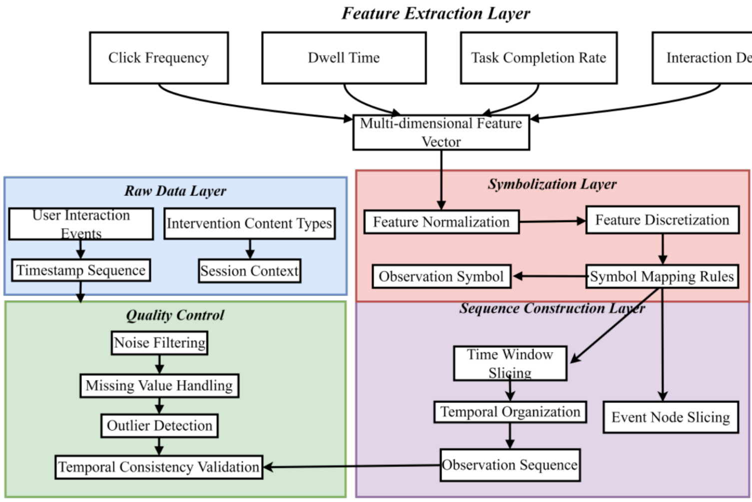

FIGURE 1. Construction of observation sequences

number of latent states [28,29]. This discretization aims to balance the expressiveness and computational feasibility of the model, while ensuring that each state has clear psychological meaning and distinguishability.

The set of latent states S contains three levels of engagement: "high compliance S1," "medium compliance S2," and "low compliance S3." In the following sections, these states are referred to as the high compliance state, the medium compliance state, and the low compliance state to enhance clarity. The definition of each of these states is as follows: "high compliance" is associated with users engaged at a high level and actively changing behaviors. Therefore, a user in this state should frequently visit, complete tasks consistently, and interact deeply. A user in "medium compliance" experiences a period of ambiguity and may exhibit some level of consistency in their behavioral traits, but not consistent with high compliance. In contrast, users in low compliance states will likely be pre-reflecting and have a high risk of dropping out and have very infrequent, shallow, or intermittent engagement patterns. The boundaries of each state and the corresponding expected behavioral characteristics are determined by domain experts based on theoretical analysis and prior empirical data to ensure content validity.

Regarding the relationship between observed symbols and latent states, as described in Section 2.1, the multidimensional behavioral feature vector is discretized to generate observed symbols. Each observed symbol is not directly and deterministically assigned to a particular latent state, but rather a probabilistic relationship is established through the observed probability matrix B of the Hidden Markov Model (HMM):

$$B = \{b_j(k)\}, \quad b_j(k) = P(o_t = v_k \mid q_t = S_j) \tag{1}$$

$b_j(k)$ is defined as the probability of generating the observation symbol v_k given the latent state S_j. Therefore, the mapping from the observation sequence to the latent state sequence is an indirect inference relationship constrained by the probabilistic model. The model automatically estimates the probability of generating various observation behavior patterns under each compliance state from the data through subsequent parameter learning. A sensitivity analysis examining the influence of the precise state definitions on model performance is presented in Section 3.7.

C. HMM PARAMETER LEARNING AND MODEL TRAINING

After completing the construction of the observation sequence and the definition of the latent state, this paper uses Hidden Markov Models (HMMs) to model the dynamic evolution of compliance [30,31]:

$$\lambda = A, B, \pi \tag{2}$$

π is the initial state probability distribution vector, representing the probability that the user is in each potential compliance state at the start of the intervention; A is the state transition probability matrix, whose elements describe the pattern of transition from one state to another, quantifying the dynamic evolution pattern of compliance level.

Since potential states cannot be directly observed, model parameters need to be estimated through a data-driven approach. This paper uses the Baum–Welch algorithm based on the expectation-maximization idea to train the model [32,33]. The algorithm's input is the set of observation sequences of all users collected from the digital platform, and iteratively maximizes the log-likelihood function of the observation sequences:

$$L(\lambda) = \sum_{n=1}^{N} \log P\left(O^{(n)} \mid \lambda\right) \tag{3}$$

In each iteration, the Baum-Welch algorithm performs two steps. First, it uses a forward-backward algorithm to calculate the posterior probability of the hidden state

[34,35]. Given the observation sequence, the probability of being in S_i at time t is:

$$\gamma_t(i) = P(q_t = S_i \mid O, \lambda) \tag{4}$$

The joint probability of a state transition occurring at adjacent time points is:

$$\xi_t(i,j) = P(q_t = S_i, q_{t+1} = S_j \mid O, \lambda) \tag{5}$$

Subsequently, in the maximization step, the model parameters are updated based on the aforementioned expected statistics:

$$\begin{cases} a_{ij} = \dfrac{\sum_{t=1}^{T-1} \xi_t(i,j)}{\sum_{t=1}^{T-1} \gamma_t(i)}, \\ \pi_i = \gamma_t(i) \end{cases} \tag{6}$$

The iterative process continues until the increase in the model's log-likelihood is lower than a preset threshold, and the optimal parameters after convergence are obtained. After training, A reveals the intrinsic law of compliance state evolution, while B characterizes the typical behavior generation patterns under different compliance levels.

D. REAL-TIME COMPLIANCE STATE DECODING AND SEQUENCE INFERENCE

After the model training is completed, a set of optimal parameters is obtained, which encapsulates the transition law between potential compliance states and their generation relationship with observed behavior. For a new user, or a new real-time behavior data stream generated during the intervention process, the core task is to infer the most likely potential state sequence behind the observed behavior sequence. This process is called decoding, which realizes the mapping from observable explicit behavior to unobservable intrinsic compliance state. This paper uses the Viterbi algorithm to complete the real-time decoding task [36]. This algorithm is an optimal path search method based on dynamic programming, and its goal is to find the state sequence with the highest probability under the given model and observation sequence. The algorithm is executed in the form of a sliding time window, which can dynamically update the inference results with the generation of new observation data, thereby meeting the real-time requirements.

The decoding process is as follows: First, initialize the variables at time t=1. For each S_i calculate its initial probability:

$$\delta_1(i) = \pi_i \cdot b_i(o_1), \quad \forall i \tag{7}$$

$\delta_1(i)$ represents the maximum probability of reaching S_i along all possible state paths up to time t, generating the observation sequence, and recording the path:

$$\psi_1(i) = 0, \quad \forall i \tag{8}$$

$\psi_1(i)$ is then used to backtrack and record the state preceding the point with the maximum probability. Subsequently, a recursive calculation is performed. For each subsequent time step t from 2 to T, and for each S_j, the following is calculated:

$$\delta_t(j) = \max_{1 \le i \le N} [\delta_{t-1}(i) \cdot a_{ij}] \cdot b_j(o_t), \quad \forall j \tag{9}$$

And recording the state i that makes the expression reach its maximum value, that is:

$$\psi_t(j) = \arg\max_{1 \le i \le N} [\delta_{t-1}(i) \cdot a_{ij}], \quad \forall j \tag{10}$$

The goal of this phase (backtracking) is to identify an individual "optimal predecessor state" for each "current state" (the present time step) as well as each time point (the previous time steps). The globally-optimal path is established through backtracking, after all of the observed sequences have been processed.

The final output sequence of "state investigators" is compiled into one trajectory that indicates how users have moved from one state of "high" to "medium" user compliance during this intervention period up until the time of intervention. Therefore, the path tracked by these "state trajectories" provides continual insight into the quality of users' engagement patterns over time.

III. MODEL PERFORMANCE AND RECOGNITION CAPABILITY EVALUATION

This chapter aims to systematically assess how well the HMM method for modeling continuous behavioural states performs in identifying adherence or compliance during psychoeducational interventions. Using the state space and parameter-learning and sequence-decoding components described in the method section, this paper performs a multi-dimensional analysis of the model's ability to identify "key turning points", state transition patterns; continuity in state sequences, interpretability, and early warning effectiveness. In addition to comparing model's output state sequence with expert-annotated results and other baseline methods, this paper will provide a comprehensive comparison of the model's output state sequence regarding its temporal consistency, structural rationality, and decision support capabilities.

A. IDENTIFICATION OF THE EVOLUTION TRAJECTORY AND KEY TURNING POINTS OF COMPLIANCE STATUS

To evaluate the Hidden Markov Model's (HMM) ability to identify key nodes in the dynamic evolution of compliance, this paper defines "key inflection points" as moments when a substantial change in state occurs. Specifically, an inflection point is operationalized as the time point at which a user's potential compliance state transitions across categories. Self-transitions during state maintenance are not considered inflection points. The evaluation benchmark was independently constructed by two researchers with over five years of experience in digital interventions in psychoeducation.

These researchers performed the annotation without access to the HMM's inference results or its parameter initialization values. Their annotations were based solely on the raw behavioral log data and a standardized coding manual derived from established psychoeducational theory, ensuring an independent reference standard for subsequent quantitative comparison. Evaluators were provided with complete time-series logs of user behavior, stripped of any model inferences, including all interaction events, timestamps, and derived features. Based on the predetermined operationalized definition and behavioral pattern paradigms, evaluators independently labeled each user with the moments when all perceived states changed throughout the intervention period, along with their preceding and following state labels. Cohen's Kappa coefficient was used to calculate inter-evaluator consistency, ensuring good consistency in the annotations presented in this paper. For discrepancies in the labeled points (approximately 7.2%), a consensus was reached through review by a third senior researcher, forming the final standard inflection point sequence.

The state sequence output from the HMM decoding was compared user-by-user with the standard inflection point sequence annotated by the experts. For a model-predicted inflection point, if the difference between its timestamp and the timestamp of an expert-annotated inflection point is within a preset tolerance window (set to ± 1 observation time unit in this paper, i.e., between two adjacent behavior slices), and the predicted state change direction (e.g., from S1 to S2) is consistent with the annotation, it is considered a correct identification (True Positive, TP). Inflection points predicted by the model but not found to match in the standard annotation are recorded as false positives (False Positive, FP), and inflection points present in the standard annotation but not predicted by the model are recorded as false negatives (False Negative, FN). To visually demonstrate the comparison between the model's identification results and expert annotations, a typical user is used as an example, and their behavior observations over time, the state sequence decoded by the HMM, the model-identified inflection points, and the expert-annotated inflection points are plotted. As shown in Figure 2, which clearly shows the continuity of the model's inferred state trajectory and the alignment of inflection point identification in the time dimension.

Figure 2 presents the behavioral observation sequence, HMM decoding state sequence, and key inflection point identification comparison of a typical user during the intervention process through four subplots. In Figure 2(a), the horizontal axis represents the observation time series, and the vertical axis represents the behavioral feature values normalized to the [0,1] interval. It shows the changes over time in click frequency (fluctuating between 0.2 and 0.8), dwell time (varying between 0.3 and 0.9), task completion rate (fluctuating between 0.15 and 0.65), and interaction depth (varying between 0.35 and 1). These features generally show a decreasing trend around time points 35 and 65, while exhibiting low-level fluctuations after time point 75, reflecting the changing process of user engagement quality. Figure 2(b) also shows the observation time series on the horizontal axis and discrete potential compliance states on the vertical axis. The state sequence decoded by the HMM shows that the user was in state S1 from time 1 to 34, in state S2 from time 35 to 65, briefly returned to state S1 from time 66 to 74, and entered state S3 from time 75 to 100. This trajectory reveals the dynamic evolution path of user compliance from high to low levels. In Figure 2(c), the inflection points are marked with red dashed lines and squares in the State Sequence of the model. These inflection points are time points 35, 66, 75, and 84. The time points 35, 66, and 75 are the locations of the change from state S1 to S2, S2 to S1 and S1 to S3. The inflection point (84) at the time, indicates that the model has identified the major state transitions, as well as some smaller fluctuations; therefore, when using the State Sequence of the model to identify inflection points in the compliance states, the model captures all major transitions in the compliance states (i.e. inflection points) and most small fluctuations. The inflection points identified by experts in Figure 2(d) are 35, 66, and 76, indicated with green dashed lines and asterisks. The experts agree with the model in identifying the first and second inflection points (i.e., time points 35 and 66). The expert mark of 76 (i.e., one time point later than the model) may be due to their different threshold of state persistence used to identify compliance states based on behavioral patterns. Overall, the expert evaluations and model results are highly consistent in identifying the same primary inflection points, supporting the conclusion that the model is able to successfully follow the evolution of compliance states over time and accurately identify the location of the primary inflection points.

B. ANALYSIS OF STATE TRANSITION PROBABILITY MATRIX AND ITS BEHAVIORAL INTERPRETATION

The model was validated to successfully capture state change nodes. A more detailed analysis of A (after training convergence) was then performed to comprehensively understand the evolution of compliance states. As described in Section 2, each element in A corresponds to the probability that an individual will transition from one compliance state to another in adjacent time slices. Quantitative analysis of A allows us to categorize the decay trajectory as either a rapid, direct decline or a gradual decline through transitional states until eventual exit from the compliance state, thus determining whether the decline in compliance is abrupt or phased. Furthermore, by combining specific observed behavioral patterns (rapid clicking and low completion rates), the difference between the transition probability under these patterns and the global transition probability is compared to assess its potential value as a risk warning signal. The analysis results are shown in Figure 3.

Figure 3 analyzes the impact of A and specific behavioral patterns through five subgraphs: Figure 3(a) presents the

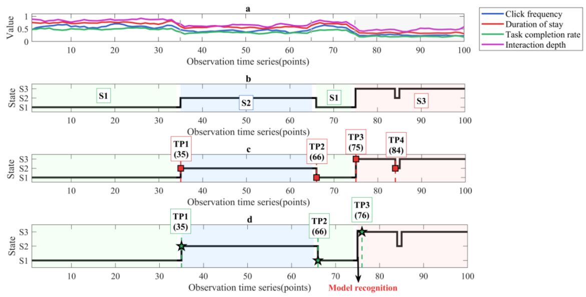
FIGURE 2. Comparison of User Compliance State Evolution and Turning Point Identification: (a) User Behavior Observation Sequence; (b) Latent Compliance State Sequence Decoded by HMM; (c) Key Turning Points Identified by the Model (Red Dashed Line); (d) Turning Points Annotated by Experts

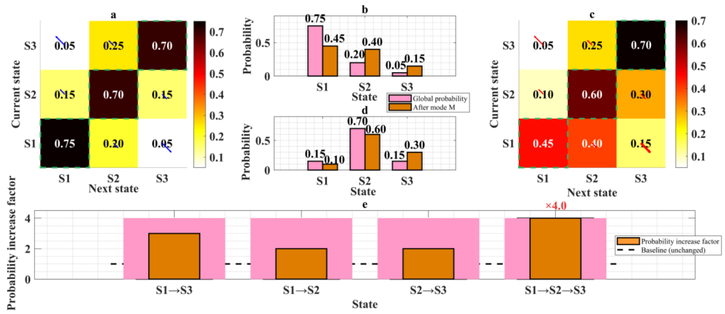
FIGURE 3. State transition probability matrix analysis and its impact on specific behavioral patterns: (a) Global state transition probability matrix; (b) Starting from S1: Global vs. Pattern M; (c) Conditional transition probability matrix under Pattern M; (d) Starting from S2: Global vs. Pattern M; (e) Increase factor of Pattern M on the probability of critical decay paths

global A in the form of a heatmap, with the horizontal and vertical axes representing the next state and the current state, respectively. The matrix elements show that the high compliance state S1 has a probability of 0.75 to remain itself, a probability of 0.20 to transfer to the medium compliance state S2, and a probability of 0.05 to directly transfer to the low compliance state S3; the medium compliance state S2 has a probability of 0.70 to remain itself, and a probability of 0.15 to transfer to S1 and S3; the low compliance state S3 has a probability of 0.70 to remain itself, a probability of 0.25 to transfer to S2, and a probability of 0.05 to transfer to S1. This indicates that each state exhibits high self-stability, and compliance decay usually requires transfer through S2. Figure 3(b) compares the global probability starting from S1 with the conditional probability after observing the "rapid clicks and low completion rate" pattern M. The data shows that when pattern M appears, the probability of staying in S1 decreases from 0.75 to 0.45, the probability of transitioning to S2 increases from 0.20 to 0.40, and the probability of directly transitioning to S3 increases from 0.05 to 0.15, indicating that this behavioral pattern significantly increases the risk of state deterioration. Figure 3(c) shows a heatmap of the conditional transition probability matrix under given pattern M. Its structure is similar to the global matrix, but the transition tendency changes. Figure 3(d) compares the case starting from S2. Under pattern M, the probability of staying in S2 decreases from 0.70 to 0.60, and the probability of transitioning to S3 increases from 0.15 to 0.30, showing that this pattern also exacerbates the decay from medium to low compliance. Figure 3(e) quantifies the multiplier of the probability increase of pattern M on the critical decay path. The probability of going directly from S1 to S3 increases by 3.0 times, from S1 to S2 by 2.0 times, and from S2 to S3 by 2.0 times. The probability of the two-step decay path from S1 to S2 to S3 increases by 4.0 times. This conclusively proves that the "fast click and low completion rate" behavior pattern is a strong predictor of compliance decay, providing a quantitative basis for early warning.

C. SMOOTHNESS AND STATE PERSISTENCE ANALYSIS OF DECODED STATE SEQUENCES

Besides the accuracy of inflection point locations, the continuity and smoothness of the compliance state sequence over time are also important aspects for evaluating model quality. If the model's output state oscillates frequently between adjacent time points, it will be difficult to reflect the true psychological evolution process and will also weaken its usability in actual intervention. Therefore, this paper analyzes the decoded state sequence from two perspectives: state duration and state switching frequency. First, the average duration of different compliance states in the test set is statistically analyzed and compared with the theoretical expected value derived based on self-transition probability to verify the stability of the model output. Second, the State Switching Frequency (SSF) and Jitter metrics are introduced to quantify the degree of fluctuation of the sequence over time. The relevant results are shown in Figure 4.

Figure 4 illustrates the smoothness and persistence of the

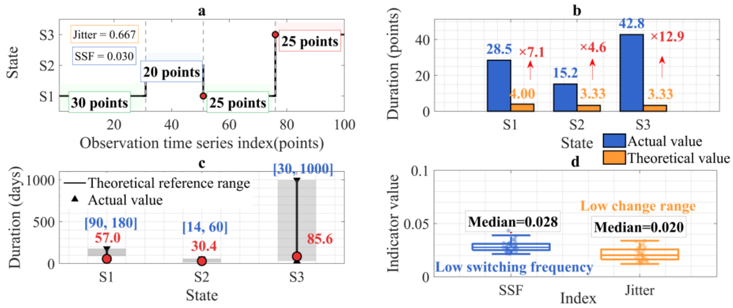

FIGURE 4. Smoothness and Durability Analysis of State Sequences: (a) Typical User State Sequence Segment (Number of State Switches: 3); (b) Actual Statistical Average Duration vs. Theoretical Estimation; (c) Actual Duration (Days) vs. Theoretical Intervention Stage Reference Range; (d) Distribution of State Sequence Smoothness Indicators for 100 Users

state sequence through four subgraphs: Figure 4(a) presents a state sequence segment of a typical user at 100 time points. The horizontal axis is the observation time series index, and the vertical axis is the compliance state (S1, S2, S3). The sequence shows four consecutive state segments—S1 lasting 30 points, S2 lasting 20 points, S1 lasting 25 points, and S3 lasting 25 points. There are only 3 state transitions during this period. The calculated SSF is 0.030 and the Jitter is 0.667, indicating that the state changes are smooth and without drastic fluctuations, which verifies the smoothness of the model output sequence. Figure 4(b) compares the actual statistical average duration (observation point) of each state with the theoretical estimate based on the self-transition probability. The actual values are S1:

28.5 points, S2: 15.2 points, and S3: 42.8 points, respectively, while the theoretical values are S1: 4.00 points,

S2: 3.33 points, and S3: 3.33 points, respectively. The actual values are significantly higher than the theoretical values, reflecting that once a state is entered, it tends to last for a long time, exceeding the duration expected by the one-step transition probability alone. In Figure 4(c), the actual durations are S1: 57.0 days, S2: 30.4 days, and S3: 85.6 days, while the theoretical reference ranges are S1: 90-180 days, S2: 14-60 days, and S3: 30-1000 days. The actual duration of S1 is 57 days, which is below the theoretical lower limit of 90 days. This discrepancy is attributed to the specific user cohort in this study, which consisted of individuals with subclinical symptoms rather than clinically diagnosed cases, resulting in a shorter sustained period of high engagement compared to theoretical models developed from clinical populations. Figure 4(d) shows the distribution of state sequence smoothness indices for 100 users. The median SSF is 0.028, and the median Jitter is 0.020. Both indices are concentrated at low levels, further confirming that most users have low state sequence switching frequency and small variation amplitude, and have high smoothness and stability overall.

D. CALCULATION OF CONTINUITY EVALUATION INDEX FOR STATE SEQUENCE INFERENCE

Based on confirming the overall smoothness of the state sequences, this paper further quantifies the model performance from the perspective of sequence-level consistency. Two metrics are introduced: State Sequence Alignment Precision (SSAA) and edit distance (which measures the minimum number of edit operations required to transform one state sequence into another, including inserting, deleting, and replacing a state label). These metrics respectively measure the consistency between the model's predicted sequence and the expert-annotated sequence at the time-point level and the overall structural level. Simultaneously, to verify the advantages of Hidden Markov Models (HMMs) in modeling temporal dependencies, they are compared with two baseline methods: a method based on artificial threshold rules (denoted by RB) and a Random Forest (RF) classification method based on sliding windows. The Random Forest method, while not inherently sequential, serves as a strong non-temporal baseline representing conventional machine learning approaches for feature-based classification, whereas the rule-based method reflects simplistic threshold-driven heuristics commonly used in practice. The three methods calculate the average SSAA and normalized edit distance on the same test set, and statistical tests are used to analyze the significance of differences. The comparison results are summarized in Figure 5.

Figure 5 provides a comprehensive evaluation of the continuity of the state sequence through four subplots: Figure 5(a) presents a heatmap showing the point-by-point alignment between the HMM predicted sequence and the expert-annotated sequence for a typical user (user #50, sequence length T=98). The horizontal axis represents time points (1 to 98), and the two rows on the vertical axis represent the alignment status (green for matching, red for mismatch) and the predicted state, respectively. The green area corresponds to a high SSAA (0.847), indicating that the model is consistent with the expert annotations at most time points. The red stripes are sparse and scattered, mainly concentrated at switching points, corresponding to a low relative edit distance (0.173). The combination of these two aspects shows that the HMM performs well in both overall accuracy and temporal continuity, and even with local biases, it does not disrupt the overall structure of the sequence. Figure 5(b) compares the average performance of the three methods using a biaxial bar chart. HMM has

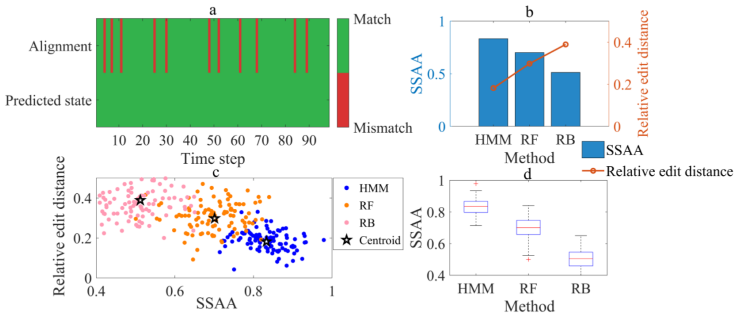

FIGURE 5. Comprehensive evaluation of state sequence continuity: (a) Point-by-point alignment of HMM predictions; (b) Average performance comparison; (c) User-level continuity and accuracy distribution; (d) Distribution of SSAA in different methods

the highest SSAA (0.833), significantly higher than RF (0.701) and RB (0.512), while its relative edit distance is the lowest (0.182), much lower than RF (0.298) and RB (0.389), indicating that HMM has the best continuity while maintaining sequence accuracy. Figure 5(c) presents the distribution of 100 users in the two-dimensional space of SSAA and relative edit distance as a scatter plot. HMM user points (blue) are densely distributed in the ideal region of SSAA>0.75 and relative edit distance<0.25, RF user points (orange) are more dispersed, and RB user points (pink) are concentrated in the region of SSAA<0.6 and relative edit distance>0.3. The center point coordinates of the three methods are (0.833,0.182), (0.701,0.298), and (0.512,0.389), respectively, which intuitively show the dual advantages of HMM in terms of continuity and accuracy. Figure 5(d) further illustrates the distribution of SSAA. The median of HMM is 0.837 with an interquartile range of [0.802, 0.874], the median of RF is 0.704 with an interquartile range of [0.662, 0.746], and the median of RB is 0.508 with an interquartile range of [0.466, 0.562]. HMM not only has the highest median but also the most concentrated distribution range, confirming that its output sequence has stable and superior continuity quality. The overall results show that HMM, by modeling the temporal dependencies between states, can generate highly smooth and accurate state sequences in the time dimension, significantly outperforming traditional methods that ignore temporal information.

E. DYNAMIC INTERPRETABILITY ANALYSIS OF COMPLIANCE BASED ON STATE TRANSITION PATTERNS

To further enhance the model's credibility in practical applications, this paper conducts an interpretability analysis of the relationship between state transition structure and observed behavioral patterns. By jointly analyzing A and B, the most representative behavioral patterns under different compliance states can be identified, and their impact on subsequent state evolution directions can be quantified. Specifically, firstly, a directed graph of state evolution is constructed to represent the main transition paths; secondly, given specific observation symbols, the expected state transition distribution is calculated and compared with the global transition structure, thereby identifying behavioral signals with significant predictive value. The results of the correlation analysis are shown in Figure 6.

Figure 6 systematically reveals the interpretable structure of the state transition pattern: The chord diagram in Figure 6(a) arranges three state nodes (S1, S2, S3) and four observation symbol nodes (v1 to v4, corresponding to "high completion rate for deep browsing", "medium completion rate for regular interaction", "low completion rate for quick clicks", and "short-term pause to skip tasks") in a circle, and the associations are represented by chords; the blue chords represent the transitions between states, and their line width is proportional to the transition probability; the colored chords represent the probability of a state generating an observation symbol, and their line width is proportional to the value in B. Intuitively, S1 is mainly strongly associated with v1 (probability 0.40), while S3 is closely related to the behaviors of v3 (probability 0.40) and v4 (probability 0.40), and the state transition chords reveal the main evolutionary direction. Figure 6(b) highlights the main evolutionary paths with a probability greater than 0.05. Among them, the blue curve shows the self-transfer paths (S1 to S1, S2 to S2, S3 to S3) with the largest flow, with probabilities of 0.75, 0.70, and 0.70, respectively, indicating that each state has high stability. Among the red curve decaying transfer paths (to lower compliance), S1 to S2 (probability 0.20) and S2 to S3 (probability 0.15) are the main paths, while the direct jump path S1 to S3 has a lower probability (0.05), indicating that compliance decay usually occurs gradually. The green curve recovering transfer paths (to higher compliance) generally have low probabilities (S3 to S2 is 0.25, S2 to S1 is 0.15, and S3 to S1 is only 0.05), revealing the difficulty of recovering from a low compliance state and indicating that there is a certain hysteresis effect in the system.

F. VALIDATION OF THE EFFECTIVENESS OF EARLY WARNING AT KEY INTERVENTION TURNING POINTS

Finally, from the perspective of practical intervention application, the performance of the HMM method in early warning of key adverse events was evaluated. Based on the state sequence decoding and risk triggering rules proposed in the methodology section, the first or sustained entry into a low compliance level was considered as a warning signal, and this was compared with traditional retrospective scale

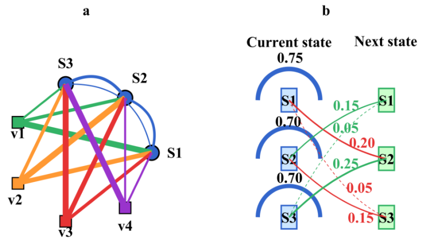

FIGURE 6. Interpretability structure analysis of state transition patterns: (a) Correlation structure between state and observation symbols; (b) Analysis of main evolutionary paths

assessment methods. By statistically analyzing the warning lead time, precision, recall, and F1 score, the efficacy difference between the two methods in predicting "significantly decreased compliance" and "intervention dropout" events was systematically evaluated. The experimental results are presented in Figure 7 and Table 1, where Figure 7 shows the distribution of the HMM's lead time relative to scale assessment, and Table 1 summarizes the key performance indicators.

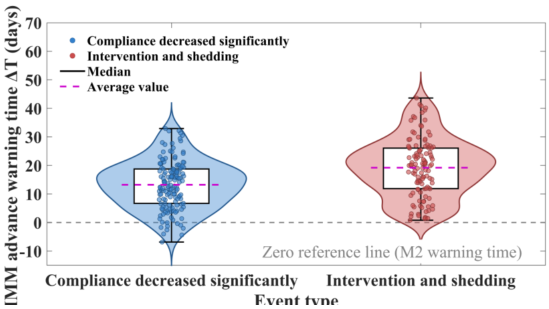

FIGURE 7. Distribution of time advance (ΔT) in HMM assessment relative to traditional scales

Figure 7 shows the distribution of the advance time (ΔT) of HMM compared to traditional scale assessment. The horizontal axis represents the two event types ("significant decline in compliance" and "intervention dropout"), and the vertical axis represents the advance time (days). The data shows that for the "significant decline in compliance" event, HMM provides an average advance warning of 12.5 days, and for the "intervention dropout" event, it provides an average advance warning of 18.2 days. Moreover, the main distribution of all ΔT values is above the zero reference line of the traditional scale assessment warning time, indicating that HMM can provide earlier warnings in most cases.

TABLE 1. Summary of Key Indicators for Early Warning Effectiveness

Evaluation Dimension	Specific Metric	HMM Method	Traditional Scale Assessment
Warning Accuracy	Precision	0.821	0.857
	Recall	0.900	0.600
	F1 Score	0.840	0.720
Comprehensive Discriminatory Ability	AUC	0.892	0.735
Decision Benefit	Proportion of Events Captured in Top 30% of Users	68.3%	42.5%

Table 1 shows that HMM significantly outperforms traditional scales in recall (0.900 vs. 0.600) and F1 score (0.84 vs. 0.72), indicating that it can capture real risk events more comprehensively. Although the scale is slightly higher in precision (0.857 vs. 0.821), HMM's comprehensive discrimination ability (AUC of 0.892 vs. 0.735) and decision benefits (capturing 68.3% of events when issuing warnings to the top 30% of users, far exceeding the scale's 42.5%) are outstanding. This confirms the comprehensive advantage of HMM in providing more timely and sensitive warnings in digital intervention, and provides a quantitative basis for real-time adaptive adjustment of intervention strategies.

G. ROBUSTNESS OF STATE DEFINITIONS

To evaluate the stability of the model's performance with respect to the operationalization of the latent compliance states, an additional analysis was conducted. A second panel of experts, independent from the original group, was asked to define an alternative set of boundaries for the high, medium, and low compliance states based on the same theoretical framework. These alternative definitions involved minor adjustments to the threshold values of the behavioral features that delineate the states. The observation sequences for all users were then relabeled according to these new state definitions, and the HMM was retrained using the same procedures described in Section 2.3. The performance of this alternative model was assessed on the test set (See Table 2).

TABLE 2. Model Performance Comparison Under Original and Alternative State Definitions

Performance Metric	Original State Definition	Alternative State Definition
State Sequence Alignment Precision	0.833	0.826
AUC	0.892	0.885
Recall for Early Warning Events	0.900	0.892
Precision for Early Warning Events	0.821	0.818
F1 Score	0.840	0.835

In Table 2, The state sequence alignment precision achieved was 0.826, compared to the original 0.833, and the area under the curve was 0.885, compared to the original 0.892. The recall for early warning events remained at 0.892, slightly below the original 0.900. These marginal differences demonstrate that the HMM's performance is robust to reasonable variations in the expert-defined state boundaries, supporting the generalizability of the findings.

IV. CONCLUSION

This research evaluates how to match psychoeducational interventions with users in a way that dynamically and continuously monitors compliance levels. The approach is based on HMM to define three distinct compliance levels – high, medium, and low. The observations used for modeling user compliance with these three states are taken from use of an online system to observe and interpret user behaviour sequences as they occur over time while implementing the psychoeducational intervention. Using the results of the experiments conducted, the earliest warning of compliance levels with users has been determined; these results also provide evidence that the tracking of users' compliance levels over time can be accurately tracked through the application and monitoring of real-time HMM decoding. This paper provides a continuous and dynamic compliance monitoring framework for psychoeducational interventions, expands the application of time-series models in the field of mental health, and facilitates refined assessment and adaptive adjustment of the intervention process.

AUTHOR CONTRIBUTIONS

This article has only one author.

CONFLICTS OF INTEREST

The authors declare that they have no financial conflicts of interest.

FUNDING

This work was supported by Hebi Polytechnic 2025 University-level Innovation Team, 2025SK01; 2025 Henan Provincial Education System Special Research Project on Integrity <Promoting the Innovation of Party Discipline Education Methods -An Exploration of the "Seven-Force-Driven and Three-Dimensional Closed-Loop" Model from the Perspective of Model Party Branch Construction>,2025LZZD-86; 2024 Henan Provincial Medical Education Research Project <Research on the Four-Dimensional Reconstruction of Labor Curriculum for Higher Vocational Nursing Major Based on Tyler's Principles Under the Background of New Medical Science>,WJLX2024233;General Project of Henan Educational Science Planning 2025 (2025YB0670)

Research and Practice Project on Education and Teaching Reform, Hebi Polytechnic (2025XJJGLX001)

Research and Practice Project on Education and Teaching Reform, Hebi Polytechnic (2025XJJGLX018)

DATA AVAILABILITY STATEMENT

The data that support the findings of this study are available from the corresponding author, upon reasonable request.

ETHICS STATEMENT AND INFORMED CONSENT

User behavior sequences collected from a digital platform are used as observations. These data are fully anonymized and de-identified prior to analysis, containing no personally identifiable information. The dataset was obtained from publicly available or platform-authorized sources and is analyzed in an aggregated manner. Therefore, the study does not involve human subjects as defined by relevant ethical guidelines, and ethical approval as well as informed consent were not required.

ACKNOWLEDGEMENTS

None.

REFERENCES

[1] P. Musiat, C. Johnson, M. Atkinson, et al., "Impact of guidance on intervention adherence in computerised interventions for mental health problems: a meta-analysis," Psychological medicine, vol. 52, no. 2, pp. 229-240, 2022, doi: 10.1017/S0033291721004621.

[2] P. Harmanci and K. Budak F, "The effect of psychoeducation based on motivational interview techniques on medication adherence, hope, and psychological well-being in schizophrenia patients," Clinical Nursing Research, vol. 31, no. 2, pp. 202-216, 2022, doi: 10.1177/10547738211046438.

[3] M. Liu and M. Schueller S, "Moving evidence-based mental health interventions into practice: implementation of digital mental health interventions," Current treatment options in psychiatry, vol. 10, no. 4, pp. 333-345, 2023, doi: 10.1007/s40501-023-00298-2.

[4] G. Woolley M, S. Klimczak K, H. Davis C, et al., "Predictors of adherence to a publicly available self-guided digital mental health intervention," Cognitive behaviour therapy, vol. 53, no. 6, pp. 577-591, 2024, doi: 10.1080/16506073.2024.2341807.

[5] R. Maqsood, P. Ceravolo, C. Romero, et al., "Modeling and predicting students' engagement behaviors using mixture Markov models," Knowledge and Information Systems, vol. 64, no. 5, pp. 1349-1384, 2022, doi: 10.1007/s10115-022-01674-9.

[6] A. Jayasree, P. Shanmuganathan, P. Ramamurthy, et al., "Types of medication non-adherence & approaches to enhance medication adherence in mental health disorders: a narrative review," Indian Journal of Psychological Medicine, vol. 46, no. 6, pp. 503-510, 2024, doi: 10.1177/02537176241233745.

[7] V. White, J. Linardon, J. E. Stone, et al., "Online psychological interventions to reduce symptoms of depression, anxiety, and general distress in those with chronic health conditions: a systematic review and meta-analysis of randomized controlled trials," Psychological Medicine, vol. 52, no. 3, pp. 548-573, 2022, doi: 10.1017/S0033291720002251.

[8] A. Shehu, H. Gommaa, U. S. Usman, et al., “Effect of Psycho-Educational Intervention on Drug Adherence and Quality of Life Among Patients With Schizophrenia in Jigawa State and Nigeria,” International Journal of Scientific Research Updates, vol. 4, no. 1, pp. 163-171, 2022, doi: 10.53430/ijsru.2022.4.1.0103.

[9] J. Buckby, T. Wang, D. Fletcher, et al., “Finding the number of latent states in hidden Markov models using information criteria,” Environmental and Ecological Statistics, vol. 30, no. 4, pp. 797-825, 2023, doi: 10.1007/s10651-023-00584-5.

[10] E. Sidrow, N. Heckman, E. Fortune S M, et al., “Modelling multiscale, state-switching functional data with hidden Markov models,” Canadian Journal of Statistics, vol. 50, no. 1, pp. 327-356, 2022, doi: 10.1002/cjs.11673.

[11] A. Maruotti, M. Fabbri, and M. Rizzolli, “Multilevel hidden Markov models for behavioral data: A Hawk-and-Dove experiment,” Multivariate Behavioral Research, vol. 57, no. 5, pp. 825-839, 2022, doi: 10.1080/00273171.2021.1912583.

[12] S. Mildiner Moraga and E. Aarts, “Go multivariate: Recommendations on bayesian multilevel hidden Markov models with categorical data,” Multivariate Behavioral Research, vol. 59, no. 1, pp. 17-45, 2024, doi: 10.1080/00273171.2023.2205392.

[13] A. Ravari, F. Ghoreishi S, and M. Imani, “Optimal inference of hidden Markov models through expert-acquired data,” IEEE Transactions on Artificial Intelligence, vol. 5, no. 8, pp. 3985-4000, 2024, doi: 10.1109/TAI.2024.3358261.

[14] A. Gupta, D. Garg, and P. Kumar, “Mining sequential learning trajectories with hidden Markov models for early prediction of at-risk students in e-learning environments,” IEEE Transactions on Learning Technologies, vol. 15, no. 6, pp. 783-797, 2022, doi: 10.1109/TLT.2022.3197486.

[15] X. Cheng and B. Huang, “CSI-based human continuous activity recognition using GMM–HMM,” IEEE Sensors Journal, vol. 22, no. 19, pp. 18709-18717, 2022, doi: 10.1109/JSEN.2022.3198248.

[16] X. Zhao, L. Huang, L. Wang, et al., “Understanding of the dynamics of mobile reading: An HMM model of user engagement and content consumption,” Production and Operations Management, vol. 34, no. 12, pp. 3755-3774, 2025, doi: 10.1111/poms.13964.

[17] X. Ye and M. Han M, “An improved feature extraction algorithm for insider threat using hidden Markov model on user behavior detection,” Information & Computer Security, vol. 30, no. 1, pp. 19-36, 2022, doi: 10.1108/ICS-12-2019-0142.

[18] M. Boeker, L. Hammer H, A. Riegler M, et al., “Prediction of schizophrenia from activity data using hidden Markov model parameters,” Neural Computing and Applications, vol. 35, no. 8, pp. 5619-5630, 2023, doi: 10.1007/s00521-022-07845-7.

[19] Q. Liu, D. Cole, T. Tran, et al., “Intraindividual phenotyping of depression in high-risk youth: An application of a multilevel hidden Markov model,” Development and psychopathology, vol. 36, no. 3, pp. 1262-1271, 2024, doi: 10.1017/S0954579423000500.

[20] J. Wu, G. Ward O, J. Curley, et al., “Markov-modulated Hawkes processes for modeling sporadic and bursty event occurrences in social interactions,” The Annals of Applied Statistics, vol. 16, no. 2, pp. 1171-1190, 2022, doi: 10.1214/21-AOAS1539.

[21] R. Jouini, C. Houaidia, and A. Saidane L, “Hidden markov model for early prediction of the elderly’s dependency evolution in ambient assisted living,” Annals of Telecommunications, vol. 78, no. 9, pp. 599-615, 2023, doi: 10.1007/s12243-023-00964-9.

[22] J. Liu, T. Yue W, M. Leung A C, et al., “Find the Good,” Seek the unity: A hidden Markov model of human-AI delegation dynamics. Mis Quarterly, vol. 49, no. 3, pp. 1185-1204, 2025, doi: 10.25300/MISQ/2024/18232.

[23] S. Faruque, A. Mizuno, L. Wang, et al., “Unique Time-Series Patterns of Behavioral and Psychological Factors in Late-Life Depression: A Computational Psychiatry Approach with Hidden Markov Models,” The American Journal of Geriatric Psychiatry, vol. 32, no. 4, pp. S50-S51, 2024, doi: 10.1016/j.jagp.2024.01.122.

[24] B. Ogbagaber S, Y. Cui, K. Li, et al., “A hidden Markov modeling approach combining objective measure of activity and subjective measure of self-reported sleep to estimate the sleep-wake cycle,” Journal of Applied Statistics, vol. 51, no. 2, pp. 370-387, 2024, doi: 10.1080/02664763.2022.2151576.

[25] K. Archambeau, J. Couto, and L. Van Maanen, “Non-parametric mixture modeling of cognitive psychological data: A new method to disentangle hidden strategies,” Behavior Research Methods, vol. 55, no. 5, pp. 2232-2248, 2023, doi: 10.3758/s13428-022-01837-0.

[26] Y. Tang, Z. Li, G. Wang, et al., “Modeling learning behaviors and predicting performance in an intelligent tutoring system: a two-layer hidden Markov modeling approach,” Interactive Learning Environments, vol. 31, no. 9, pp. 5495-5507, 2023, doi: 10.1080/10494820.2021.2010100.

[27] X. Tang, “A latent hidden Markov model for process data,” psychometrika, vol. 89, no. 1, pp. 205-240, 2024, doi: 10.1007/s11336-023-09938-1.

[28] B. Gardner, A. Arden M, D. Brown, et al., “Developing habit-based health behaviour change interven tions: Twenty-one questions to guide future research,” Psychology & health, vol. 38, no. 4, pp. 518-540, 2023, doi: 10.1080/08870446.2021.2003362.

[29] A. Abrash Walton, L. Nageotte N, E. Heimlich J, et al., “Facilitating behavior change: Introducing the Transtheoretical Model of Behavior Change as a conservation psychology framework and tool for practitioners,” Zoo Biology, vol. 41, no. 5, pp. 386-397, 2022, doi: 10.1002/zoo.21704.

[30] R. Colombi, S. Giordano, and M. Kateri, “Hidden markov models for longitudinal rating data with dynamic response styles,” Statistical Methods & Applications, vol. 33, no. 1, pp. 1-36, 2024, doi: 10.1007/s10260-023-00717-x.

[31] Y. Liu, A. Culpepper S, and Y. Chen, “Identifiability of hidden Markov models for learning trajectories in cognitive diagnosis,” psychometrika, vol. 88, no. 2, pp. 361-386, 2023, doi: 10.1007/s11336-023-09904-x.

[32] S. Zhang, T. Yang L, Y. Zhang, et al., “Tensor-Based Baum–Welch Algorithms in Coupled Hidden Markov Model for Responsible Activity Prediction,” IEEE Transactions on Computational Social Systems, vol. 10, no. 6, pp. 2924-2937, 2023, doi: 10.1109/TCSS.2022.3227458.

[33] B. Benyacoub, S. ElBernoussi, A. Zoglat, et al., “Credit scoring model based on HMM/Baum-Welch method,” Computational Economics, vol. 59, no. 3, pp. 1135-1154, 2022, doi: 10.1007/s10614-021-10122-9.

[34] M. Ouzineb and B. Benyacoub, “Hidden Markov Models Training Using Hybrid Baum Welch-Variable Neighborhood Search Algorithm,” Statistics, Optimization & Information Computing, vol. 10, no. 1, pp. 160-170, 2022, doi: 10.19139/soic-2310-5070-1213.

[35] V. Rezaei Tabar, D. Plewczynski, and H. Fathipor, “Generalized baum-welch and viterbi algorithms based on the direct dependency among observations,” Journal of the Iranian Statistical Society, vol. 17, no. 2, pp. 205-225, 2022, doi: 10.29252/jirss.17.2.10.

[36] J. Lember, “Local Viterbi property in decoding,” Information and Inference: A Journal of the IMA, vol. 12, no. 3, pp. 1267-1294, 2023, doi: 10.1093/imaiai/iaad004.